JB Accepted Manuscript Posted Online 11 October 2021
J Bacteriol doi:10.1128/JB.00350-21
Copyright © 2021 American Society for Microbiology. All Rights Reserved.

Accepted Manuscript Posted Online
Journal of Bacteriology
JB
Journal of Bacteriology

J. Bacteriol.

Regulatory small RNA, Qrr2, is expressed independently of sigma factor-54 and can function as the sole Qrr sRNA to control quorum sensing in *Vibrio parahaemolyticus*

Tague, J.G., J. Hong, S.S. Kalburge, and E.F. Boyd*

Department of Biological Sciences, University of Delaware, Newark, DE, 19716

Corresponding author*

Dr. E. Fidelma Boyd

Department of Biological Sciences

University of Delaware

Newark, DE 19716

Phone: (302) 831-1088. Fax: (302) 831-2281 Email: fboyd@udel.edu

Downloaded from https://journals.asm.org/journal/jb on 25 October 2021 by 132.174.254.72.

Accepted Manuscript Posted Online

18 **Abstract**

19 Bacterial cells alter gene expression in response to changes in population density in a
20 process called quorum sensing (QS). In *Vibrio harveyi*, LuxO, a low cell density activator
21 of sigma factor-54 (RpoN), is required for transcription of five non-coding regulatory
22 sRNAs, Qrr1-Qrr5, which each repress translation of the master QS regulator LuxR.
23 *Vibrio parahaemolyticus*, the leading cause of bacterial seafood-borne gastroenteritis, also
24 contains five Qrr sRNAs that control OpaR (the LuxR homolog), controlling capsule
25 polysaccharide (CPS), motility, and metabolism. We show that in a Δ*luxO* deletion
26 mutant, *opaR* was de-repressed and CPS and biofilm were produced. However, in a
27 Δ*rpoN* mutant, *opaR* was repressed, no CPS was produced, and less biofilm production
28 was observed compared to wild type. To determine why *opaR* was repressed,
29 expression analysis in Δ*luxO* showed all five *qrr* genes were repressed, while in Δ*rpoN*
30 the *qrr2* gene was significantly de-repressed. Reporter assays and mutant analysis
31 showed Qrr2 sRNA can act alone to control OpaR. Bioinformatics analysis identified a
32 sigma-70 (RpoD) -35 -10 promoter overlapping the canonical sigma-54 (RpoN) -24 -12
33 promoter in the *qrr2* regulatory region. The *qrr2* sigma-70 promoter element was also
34 present in additional *Vibrio* species indicating it is widespread. Mutagenesis of the
35 sigma-70 -10 promoter site in the Δ*rpoN* mutant background, resulted in repression of
36 *qrr2*. Analysis of *qrr* quadruple deletion mutants, in which only a single *qrr* gene is
37 present, showed that only Qrr2 sRNA can act independently to regulate *opaR*. Mutant

Journal of Bacteriology JB Journal of Bacteriology

Downloaded from https://journals.asm.org/journal/jb on 25 October 2021 by 132.174.254.72.

Accepted Manuscript Posted Online

Journal of Bacteriology

JB

and expression data also demonstrated that RpoN and the global regulator, Fis, act additively to repress *qrr2*. Our data has uncovered a new mechanism of *qrr* expression and shows that Qrr2 sRNA is sufficient for OpaR regulation.

Importance

The quorum sensing non-coding sRNAs are present in all *Vibrio* species but vary in number and regulatory roles among species. In the Harveyi clade, all species contain five *qrr* genes, and in *V. harveyi* these are transcribed by sigma-54 and are additive in function. In the Cholerae clade, four *qrr* genes are present, and in *V. cholerae* the *qrr* genes are redundant in function. In *V. parahaemolyticus*, *qrr2* is controlled by two overlapping promoters. In an *rpoN* mutant, *qrr2* is transcribed from a sigma-70 promoter that is present in all *V. parahaemolyticus* strains and in other species of the Harveyi clade suggesting a conserved mechanism of regulation. Qrr2 sRNA can function as the sole Qrr sRNA to control OpaR.

Downloaded from https://journals.asm.org/journal/jb on 25 October 2021 by 132.174.254.72.

Accepted Manuscript Posted Online

Journal of Bacteriology

JB

Journal of Bacteriology

Introduction

Bacteria monitor changes in cell density using a process termed quorum sensing (QS) (1, 2). QS is a regulatory mechanism used to alter global gene expression in response to cell density changes (1-6). In many Gram-negative bacteria, N-acylhomoserine lactone (AHL) is a common QS autoinducer synthesized intracellularly and secreted out of the cell (2, 7). By surveying AHL levels in its environment, a bacterium can regulate gene expression in response to growth phase. Quorum sensing has been characterized in several marine species in the genus *Vibrio*, including *V. anguillarum, V. cholerae, V. harveyi* and *V. parahaemolyticus*, and shown to modulate expression of bioluminescence, capsule formation, biofilm, natural competence, swarming motility, and virulence (5, 7-20). Many of the original QS studies were performed in *Vibrio harveyi* ATCC BAA-1116 aka BB120, however this strain has been reclassified as *V. campbellii*, but to avoid confusion with published literature we will continue to use the name *V. harveyi* (21). In *V. harveyi* and *V. anguillarum*, it was shown that LuxO, the QS response regulator, is an activator of sigma factor-54, encoded by *rpoN* that along with RNA polymerase, initiates transcription of the non-coding quorum regulatory small RNAs (Qrr) (8, 22, 23).

Non-coding sRNAs are a group of regulators present in prokaryotes that together with the RNA chaperone Hfq control gene expression in a range of phenotypes (24-26). The Qrr sRNAs are classified as *trans*-acting sRNAs that along with Hfq, target mRNA via base-pairing to the 5′ UTR to stabilize or destabilize translation (27-29). In *V.*

Downloaded from https://journals.asm.org/journal/jb on 25 October 2021 by 132.174.254.72.

Accepted Manuscript Posted Online

Journal of Bacteriology

JB

harveyi, the nucleoid structuring protein Fis was shown to be a positive regulator of *qrr* gene expression (30). The Qrr sRNAs are post-transcriptional regulators that, in *V. harveyi*, enhanced translation of the QS low cell density (LCD) master regulator AphA and inhibited translation of the QS high cell density (HCD) master regulator LuxR (28, 31-33). At HCD in *V. harveyi*, LuxO is not phosphorylated and therefore cannot activate sigma-54 (RpoN), the five Qrr sRNA genes *qrr1* to *qrr5* are repressed, and LuxR translation is de-repressed. In addition, AphA and LuxR repress each other transcriptionally, providing a further level of regulation (32, 34-36). Studies have shown that in *V. harveyi*, Qrr1 has a 9-bp deletion in the 5′ region of the sRNA and therefore cannot activate *aphA* translation but can still repress *luxR* translation. The deletion in *qrr1* is also present in *V. cholerae, V. parahaemolyticus* and several other *Vibrio* species (32, 37). In *V. harveyi*, Qrr2, Qrr3, Qrr4, and Qrr5 sRNAs were additive in function and controlled the same target sites (27, 28, 38). However, the *qrr* genes showed distinct expression patterns and controlled the QS output signal at different levels coordinated with highest to lowest expression: Qrr4 > Qrr2 > Qrr3 > Qrr1 > Qrr5 (28). *V. cholerae* encodes four Qrr sRNAs, Qrr1 to Qrr4 that were redundant in function with any one of the four Qrr sRNAs sufficient to repress HapR (the LuxR homolog) (27).

Vibrio parahaemolyticus (VP) is a halophile, residing in marine environments as a free-living organism or in association with marine flora and fauna (39-41). This species is the leading cause of seafood-borne bacterial gastroenteritis worldwide, causing

Downloaded from https://journals.asm.org/journal/jb on 25 October 2021 by 132.174.254.72.

Journal of Bacteriology

Accepted Manuscript Posted Online

Journal of Bacteriology

JB

increasing infections each year, and is also a serious pathogen in the aquaculture industry (42, 43). *Vibrio parahaemolyticus* has dual flagellar systems, with the lateral flagellum system required for swarming motility, an important multicellular behavior (44). *Vibrio parahaemolyticus* has the same QS components and pathway as *V. harveyi*, containing five Qrr sRNAs that are predicted to control *aphA* and *opaR* (Fig. 1). In this species, the LuxR homolog is named OpaR (Opacity Regulator), for its role as an activator of capsule polysaccharide (CPS) production that results in an opaque, rugose colony morphology (45). The McCarter group first showed that an *opaR* deletion mutant in strain BB22OP had a translucent, smooth colony morphology, reduced CPS and biofilm (46). A further study by the same group also showed that Δ*opaR* produced less biofilm when grown statically at 30°C for 16h, but showed similar biofilm levels at 24h and more biofilm than wild type after 48h growth (20). In *V. parahaemolyticus* RIMD2210633, Δ*opaR* also showed a defect in CPS and biofilm, but the biofilm defect disappeared after 24h growth (14). A recent study in this same strain proposed that *opaR* was a negative regulator of biofilm through modulation of c-di-GMP, although the method and time point examined differed with the previous study (47). A third strain, HZ, with a deletion in *opaR* also showed a defect in biofilm compared to wild type at both 24h and 48h (48). These data indicate that the role of CPS production in biofilm formation is complex as has been shown for other *Vibrio* species and is influenced by the methods and time points used (49-52). Besides CPS and biofilm formation, OpaR was

Downloaded from https://journals.asm.org/journal/jb on 25 October 2021 by 132.174.254.72.

Accepted Manuscript Posted Online

Journal of Bacteriology

JB

Journal of Bacteriology

shown to regulate swimming and swarming motility, surface sensing, metabolism, and the osmotic stress response in this species (14, 15, 20, 53-56). A *V. parahaemolyticus* Δ*luxO* deletion mutant, in which the *qrr* sRNAs were not expressed, showed *opaR* was highly induced and produced both CPS and biofilm, output signals of the QS pathway (14). Interestingly, an earlier study examining an Δ*rpoN* deletion mutant in *V. parahaemolyticus* showed that it did not produce CPS and generated less biofilm compared to wild type (57). This is unexpected because previous studies in *V. harveyi* suggest that in a Δ*rpoN* mutant, the *qrr* sRNA were repressed and the *luxR* (*opaR* homolog) was de-repressed inducing bioluminescence (8). In *V. parahaemolyticus,* OpaR is a positive regulator of the CPS biosynthesis operon and therefore we expect that in a Δ*rpoN* mutant CPS should be produced.

Here, we examined mutants of the QS pathway in *V. parahaemolyticus* to determine why the QS pathway output phenotypes differ between the Δ*luxO* and Δ*rpoN* mutants. We examined single and double mutants of Δ*luxO* and Δ*rpoN* for CPS and biofilm formation. Then, we determined the expression patterns of *opaR, aphA* and the five *qrr* genes in these mutants. Data showed that *qrr2* was de-repressed in the Δ*rpoN* mutant and *opaR* was repressed. Bioinformatics analysis of the *qrr2* regulatory region identified a RpoD -35 -10 promoter region that overlapped with the RpoN -24 -12 promoter, suggesting a mechanism by which *qrr2* is expressed in the Δ*rpoN* mutant. We performed mutagenesis analysis of the RpoD promoter to examine this further. To

Downloaded from https://journals.asm.org/journal/jb on 25 October 2021 by 132.174.254.72.

Accepted Manuscript Posted Online

Journal of Bacteriology

JB

Journal of Bacteriology

determine whether the other Qrr sRNAs can also function independently, we constructed quadruple *qrr* mutants, in which only one *qrr* is present, and examined CPS and motility phenotypes. Using a DNA affinity pulldown assay, we identified several potential novel regulators of *qrr2*. One of these, Fis, was examined further to determine its role in *qrr2* expression. We preformed sequence comparative analysis of the promoter regions of *qrr2* among several species within the Harveyi clade to determine if presence of an RpoD promoter is prevalent. Overall, our data showed that Qrr2 can function solely to control OpaR and has a novel mechanism of expression in *V. parahaemolyticus*.

Results:

Differential expression of *opaR* and *aphA* in Δ*luxO* versus Δ*rpoN* mutants. We used CPS production as a readout of OpaR presence in the *V. parahaemolyticus* cell. Based on the quorum sensing pathway in *V. harveyi*, we would expect both a Δ*luxO* and Δ*rpoN* deletion mutant to produce CPS, as the Qrr sRNAs should be repressed, and therefore OpaR should be de-repressed (**Fig. 1**). In a CPS assay, the Δ*luxO* mutant produced CPS forming opaque, rugose colonies. However, the Δ*rpoN* mutant did not produce CPS, and instead formed a translucent, smooth colony morphology, similar to the Δ*opaR* strain (**Fig. 2A**). Complementation of Δ*rpoN* with a functional copy of *rpoN* from an expression plasmid restored the CPS phenotype and similarly complementation of Δ*opaR* with a functional copy of *opaR* restored CPS production (Fig. S1A and S1B). In

Downloaded from https://journals.asm.org/journal/jb on 25 October 2021 by 132.174.254.72.

Accepted Manuscript Posted Online

Journal of Bacteriology

JB

addition, a Δ*rpoN*/Δ*luxO* double mutant also lacked CPS and produced a translucent, smooth colony morphology. Similarly, when we examined biofilm formation, both the Δ*rpoN* and Δ*rpoN*/Δ*luxO* double mutant strains produced less biofilm than the wild type and Δ*luxO* strains (**Fig. 2B**). These data suggest that in the Δ*rpoN* mutant, *opaR* is repressed. To test this, we complemented the Δ*rpoN* mutant with the *opaR* gene (pBAD*opaR*), and in these cells CPS production was restored, indicating that the absence of *opaR* in the Δ*rpoN* mutant led to the CPS defect (**Fig. S1C**).

Next, we investigated the expression profiles of the QS master regulators in the Δ*luxO* and Δ*rpoN* deletion mutants. RNA isolation and quantitative real-time PCR (qPCR) assays were performed from cells grown in LB 3% NaCl to optical densities (OD) 0.1 and 0.5. At OD 0.1, expression of *opaR* in Δ*luxO* relative to wild type was significantly upregulated, however, *opaR* expression was unchanged in the Δ*rpoN* mutant (**Fig. 3A**). At OD 0.5, expression of *opaR* in Δ*luxO* matched that of wild type, however, in the Δ*rpoN* mutant expression of *opaR* was significantly downregulated relative to wild type (**Fig. 3B**). Expression of *aphA*, the low cell density QS master regulator, was repressed in the Δ*luxO* mutant compared to wild type and unchanged in the Δ*rpoN* mutant at OD 0.1 (**Fig. 3C**). At OD 0.5, *aphA* expression was upregulated compared to wild type in Δ*rpoN* (**Fig. 3D**). These data indicate that *opaR* is repressed and *aphA* is induced in the Δ*rpoN* deletion mutant.

Downloaded from https://journals.asm.org/journal/jb on 25 October 2021 by 132.174.254.72.

Accepted Manuscript Posted Online

Journal of Bacteriology

JB

Expression analysis of *qrr1* to *qrr5* in Δ*luxO* and Δ*rpoN* mutants. Since *opaR* showed different levels of expression in the Δ*luxO* and Δ*rpoN* deletion mutants, we wanted to determine whether this was due to differences in *qrr* expression levels. We examined expression of all five *qrr* genes in cells grown to OD 0.1 and OD 0.5 and show that the expression of *qrr1, qrr2, qrr3* and *qrr5* was higher at OD 0.1 relative to OD 0.5 (**Fig. S2)**. Expression of *qrr4* was detected at OD 0.1, but was not detected at OD 0.5 in wild type. In addition, *qrr4* expression was not detected in either Δ*luxO* or Δ*rpoN* at OD 0.1 or 0.5 indicating that it has a strict requirement for LuxO and RpoN, but expression of *qrr4* in WT at 0.1 OD matched expression of the other *qrr* genes. This suggests that the main role of *qrr4* could be regulation at low cell density. Next, we examined expression of the *qrr* genes at OD 0.1 in the Δ*luxO* mutant relative to wild type and showed *qrr1* expression was unchanged, but there was significant downregulation of *qrr2, qrr3,* and *qrr5* (**Fig 4A**). Whereas at OD 0.5, their expression matched that of wild type (**Fig. 4B**). In the Δ*rpoN* mutant, expression of *qrr1, qrr3*, and *qrr5* matched that of the Δ*luxO* mutant (**Fig. 4C**), however, *qrr2* was upregulated at both OD 0.1 and OD 0.5 (**Fig. 4D**). To confirm that *qrr2* was differentially regulated between Δ*luxO* and Δ*rpoN*, the *qrr2* regulatory region was cloned into the pRU1064 reporter vector upstream of a promoter-less *gfp* cassette (P*qrr2-gfp*). The specific fluorescence of P*qrr2-gfp* was examined in the wild type, Δ*luxO,* and Δ*rpoN* mutants and measured as a cumulative read-out of *qrr2* transcription (**Fig. 5A**). The level of specific fluorescence of P*qrr2-gfp* was reduced in the

Downloaded from https://journals.asm.org/journal/jb on 25 October 2021 by 132.174.254.72.

Accepted Manuscript Posted Online

Journal of Bacteriology

JB

193 Δ*luxO* mutant relative to wild type, whereas in the Δ*rpoN* mutant, fluorescence was
194 significantly increased (**Fig. 5A**). Next, we examined the *opaR* regulatory region cloned
195 into pRU1064 reporter vector upstream of a promoter-less *gfp* cassette (P*opaR-gfp*) in
196 wild type, a Δ*qrr2* single mutant and a Δ*qrr3,1,4,5* quadruple mutant with only *qrr2*
197 present (**Fig. 5B**). In Δ*qrr2* compared to wild type, P*opaR-gfp* showed significantly
198 increased fluorescence, whereas the quadruple *qrr* deletion mutant, with *qrr2* present,
199 was similar to wild type (**Fig. 5B**). We predicted that deletion of *qrr2* in the Δ*rpoN*
200 mutant background should restore *opaR* expression and CPS production. We
201 constructed a Δ*rpoN*/Δ*qrr2* double mutant and examined *opaR* and *aphA* expression
202 levels (**Fig. S3)**. Quantitative real time PCR assays showed that *opaR* was highly
203 expressed in a Δ*rpoN*/Δ*qrr2* double mutant compared to wild type (**Fig. S3**).
204 Examination of CPS formation showed that the Δ*rpoN*/Δ*qrr2* double mutant produced a
205 rough colony morphology (**Fig. S4A**). Similarly, in biofilm assays, the Δ*rpoN* mutant
206 produced a significantly reduced biofilm, whereas the Δ*rpoN*/Δ*qrr2* double mutant
207 produced a biofilm similar to wild type (**Fig. S4B**). Overall, these data demonstrate that
208 Qrr2 sRNA is present in the Δ*rpoN* deletion mutant and Qrr2 sRNA can function alone
209 to control OpaR and QS phenotypes.
210 **Overlapping sigma-70 and sigma-54 promoters.** The expression of *qrr2* in the Δ*rpoN*
211 mutant background indicates that an additional sigma factor can initiate *qrr2*
212 transcription. To examine this further, the regulatory regions of *qrr1* to *qrr5* in *V.*

Downloaded from https://journals.asm.org/journal/jb on 25 October 2021 by 132.174.254.72.

Accepted Manuscript Posted Online

Journal of Bacteriology

JB

Journal of Bacteriology

213 *parahaemolyticus* RIMD2210633 were aligned and surveyed for the presence of
214 additional promoter regions using the Virtual footprint promoter analysis program and
215 manual scanning of sequences. Although the five Qrr sRNAs share homology, their
216 regulatory regions are divergent with the exception of the sigma-54 canonical -24
217 (T**TGGC**A) and -12 (AAT**GCA**) promoter sites, with nucleotides in bold conserved
218 amongst all five *qrr* regulatory regions (**Fig. S5**). In the regulatory region of *qrr2*,
219 promoter analysis identified a housekeeping sigma-70 (RpoD) -35 (TTGAAA) and -10
220 (ATAATA) promoter (**Fig. 6A**). The putative sigma-70 promoter overlapped with the
221 sigma-54 -24 and -12 promoter (**Fig. 6A**), and was absent from the regulatory regions of
222 *qrr1, qrr3, qrr4,* and *qrr5* (**Fig. S5**). This suggested that *qrr2* can be transcribed by either
223 sigma-54 or sigma-70 and could explain its expression in the absence of *rpoN*. To
224 examine this further, we mutated three base-pairs of the putative sigma-70 -10
225 ATAATA site to ATACCC in the pRUP*qrr2* reporter vector (**Fig. 6A**). The mutagenized
226 vector, pRUP*qrr2*-10CCC, was conjugated into wild type and Δ*rpoN* and specific
227 fluorescence was determined. The Δ*rpoN* pRUP*qrr2*-10CCC strain showed significantly
228 reduced fluorescence relative to Δ*rpoN* pRUP*qrr2*, indicating that this site is required for
229 *qrr2* transcription in the absence of RpoN (**Fig. 6B**). The data suggests that *qrr2* can be
230 transcribed by two sigma factors using dual overlapping promoters, suggesting a
231 unique mode of regulation for Qrr2 sRNA. Comparisons of the *qrr2* regulatory region
232 among Harveyi clade species *V. alginolyticus, V. campbellii, V. harveyi,* and *V.*

Downloaded from https://journals.asm.org/journal/jb on 25 October 2021 by 132.174.254.72.

Accepted Manuscript Posted Online

Journal of Bacteriology

JB

parahaemolyticus showed that the sigma-70 promoter -10 region was highly conserved among these species (**Fig. S6**). Each of the five Qrr sRNAs also shared homology among these species (**Fig. 7**). The *qrr1* gene among all four species showed high homology clustering closely together on the phylogenetic tree but were distantly related to the other four *qrr* genes. The *qrr3* and *qrr4* genes each clustered tightly together on the tree whereas *qrr2* and *qrr5* each showed divergence among the species (**Fig. 7**). Overall divergence in regulatory regions and gene sequence amongst the *qrr* genes likely suggests differences in how each *qrr* gene is regulated and differences in the target genes of each Qrr sRNA.

Qrr2 sRNA can function independent of the other Qrr sRNAs. Next, we determined whether Qrr2 sRNA has a distinct role in this species and whether any of the four other *qrr* genes can act alone. Using a *qrr1* to *qrr5* quintuple deletion mutant (Δ*qrr*-null) and five quadruple *qrr* deletion mutants, each containing a single *qrr*, we examined several QS phenotypes (**Fig. 8**). In swarming motility assays, the Δ*qrr*-null strain was swarming deficient, as swarming is negatively regulated by OpaR **(Fig. 8A)**. In addition, four quadruple mutants, Δ*qrr3*/Δ*qrr2*/Δ*qrr4*/Δ*qrr5*; Δ*qrr2*/*qrr1* /Δ*qrr4*/Δ*qrr5*; Δ*qrr3*/Δ*qrr2*/Δ*qrr1*/*qrr5*; and Δ*qrr3*/Δ*qrr2*/Δ*qrr1*/Δ*qrr4* were all swarming deficient indicating that Qrr1, Qrr3, Qrr4 and Qrr5 sRNAs cannot function independently to control OpaR (**Fig. 8A)**. In swarming motility assays, the Δ*qrr3*/Δ*qrr1*/Δ*qrr4*/Δ*qrr5* mutant that contained only *qrr2*, behaved similar to wild type and was swarming proficient

Downloaded from https://journals.asm.org/journal/jb on 25 October 2021 by 132.174.254.72.

Accepted Manuscript Posted Online

Journal of Bacteriology

JB

Journal of Bacteriology

indicating repression of *opaR* **(Fig. 8A)**. In swimming assays, the quadruple mutants that lacked *qrr2* produced similar results to the null mutant with defects in swimming (**Fig. 8B)**. Whereas only the mutant that contained only *qrr2* showed swimming motility similar to wild type (**Fig. 8B**). Additionally, in CPS assays, the *qrr2* positive strain also showed a colony morphology similar to wild type (**Fig. 8C**). Analysis of a single *qrr2* deletion mutant indicates that it is not essential for CPS production or swarming and that the other *qrr* genes can function to control *opaR* in the absence of *qrr2* (**Fig. S7**). In summary, these data demonstrate that only Qrr2 sRNA can function independently in *V. parahaemolyticus*.

RpoN and Fis are not required for *qrr2* expression. In order to identify additional regulators of *qrr2* transcription, a DNA-affinity pull-down was performed. We used Δ*rpoN* cell lysate grown to OD 0.5 and P*qrr2* bait DNA. We identified a number of candidate regulators previously shown to bind to the *qrr* sRNA regulatory regions in *V. harveyi* (30, 36, 58) (**Fig. S8 and S9**). We decided to examine the nucleoid associated protein Fis further since it is known to be a positive regulator of *qrr* sRNA expression and binds to the *qrr* sRNA regulatory regions in both *V. harveyi* and *V. parahaemolyticus* (30, 59). The *qrr2* regulatory region shows at least three Fis binding sites containing the conserved Fis binding motif previously described in *V. parahaemolyticus* (59). A Fis binding site was located adjacent to the -35 promoter site, as well as two additional Fis binding sites, at 193-bp and 229-bp upstream of the *qrr2* transcriptional start site (**Fig.**

Downloaded from https://journals.asm.org/journal/jb on 25 October 2021 by 132.174.254.72.

Accepted Manuscript Posted Online

Journal of Bacteriology

JB

Journal of Bacteriology

9A). To confirm these Fis binding sites, we constructed three DNA probes of the *qrr2* regulatory region to use in electrophoretic shift mobility assays (EMSAs) with purified Fis protein. DNA probe 1A encompassing a single binding site showed binding and similarly Fis bound to probe 1C which contained two Fis binding sites, both probes bound in a concentration dependent manner **(Fig. 9B**). Probe 1B, which did not have a putative Fis binding site, showed weak likely non-specific binding. Next, we examined expression of the P*qrr2-gfp* reporter in wild type, Δ*rpoN* and a Δ*rpoN*/Δ*fis* double mutant and confirmed that expression of P*qrr2-gfp* was upregulated in the Δ*rpoN* mutant but was even more highly upregulated in the Δ*rpoN*/Δ*fis* double mutant (**Fig. 9C**). These data indicate that both Fis and RpoN can act as repressors of *qrr2* in *V. parahaemolyticus*, and Fis likely plays a role in enhancing sigma-54 binding.

Discussion

In this study, we investigated the role of sigma-54, LuxO, and the five Qrr sRNAs in the *V. parahaemolyticus* QS pathway and showed that the QS pathway can function in the absence of sigma-54, *qrr1*, *qrr3*, *qrr4*, or *qrr5*. This observation reflects the idea that strains and species have different expression patterns of the *qrr* sRNAs under different growth conditions and each *qrr* gene is likely controlled by different factors. Our data demonstrated that in a Δ*rpoN* mutant, cells had a defect in CPS and biofilm formation, QS phenotypes that differed from the Δ*luxO* mutant. The data showed that Qrr2 is highly expressed in a Δ*rpoN* mutant and that Qrr2 can act independent of the other Qrr

Downloaded from https://journals.asm.org/journal/jb on 25 October 2021 by 132.174.254.72.

Accepted Manuscript Posted Online

Journal of Bacteriology

JB

sRNAs to repress OpaR and QS phenotypes. In a Δ*rpoN*/Δ*qrr2* double mutant, *opaR* was de-repressed and CPS and biofilm formation were restored. Bioinformatics analysis identified a putative -35 -10 promoter region within the *qrr2* regulatory region and mutagenesis of the -10 promoter sites resulted in repression of *qrr2*. Overall, the data indicate that *qrr2* can be expressed from two promoters and this ability is likely present in other related species. There have been other accounts of sigma-54-dependent genes showing increased transcription in the absence of *rpoN* (60, 61). In these cases, a putative sigma-70 promoter was present, suggesting a potential competition for promoter sites (60, 61). For example, in *E. coli*, *glmY* a coding sRNA contained overlapping sigma-54 and sigma-70 promoters, which were shown to allow for precise control of *glmY* expression within the cell (62). In our study, we identified a sigma-70 promoter that overlaps with the sigma-54 consensus promoter sequence of *qrr2*, suggesting that RpoN under differ growth conditions may block RpoD access. We propose that in the wild type background, *qrr2* is transcribed via LuxO activated RpoN, and in the Δ*luxO* mutant, *qrr2* is not transcribed because sigma-54 is in an inactive state bound to the *qrr2* promoter. RpoN physically blocking additional sigma factors from binding was previously proposed from studies in other bacteria (63, 64). However, in the absence of sigma-54, sigma-70 is able to bind to the *qrr2* regulatory region at a conserved -35 and -10 region to initiate transcription (**Fig. 10**). Fis is a global regulator that is known to enhance and inhibit transcription from promoter regions in many

Downloaded from https://journals.asm.org/journal/jb on 25 October 2021 by 132.174.254.72.

Accepted Manuscript Posted Online

Journal of Bacteriology

JB

bacterial species (65-68). In *V. parahaemolyticus*, Fis was shown to positively regulate *qrr* sRNAs expression. The *fis* gene was shown to be highly expressed in exponential growth only and Fis bound to the regulatory region of all five *qrr* sRNA genes (59). Here, we show in DNA protein binding assays in *V. parahaemolyticus* that Fis binds adjacent to the -35 promoter site. We speculate that Fis functions to enhance RpoN promoter binding to maximize *qrr* expression. The data showed that in the absence of both RpoN and Fis, however, *qrr2* expression is significantly increased compared to the Δ*rpoN* mutant alone. Under these conditions additional binding sites within the *qrr2* regulatory region may be fully exposed, allowing sigma-70 full access for increased *qrr2* expression (**Fig. 10)**. Our previous study has shown that in a Δ*fis* deletion mutant *qrr2* expression is repressed suggesting that Fis may also block sigma-70 binding in exponential phase cells (59). A study in *V. alginolyticus* MVP01, a species closely related to *V. parahaemolyticus*, also showed differences between the Δ*luxO* and Δ*rpoN* mutant strains in their control of cell density dependent siderophore production. The Δ*luxO* mutant showed reduced siderophore production, which is negatively regulated by LuxR, and the Δ*rpoN* mutant showed increased production (69). Their data showed RpoN dependent and independent siderophore production. We speculate that this could be the result of expression by RpoD since *V. alginolyticus* has an RpoD -35 -10 promoter in the Qrr2 regulatory region (**Fig. S6**).

Downloaded from https://journals.asm.org/journal/jb on 25 October 2021 by 132.174.254.72.

Accepted Manuscript Posted Online

Journal of Bacteriology

JB

In *V. cholerae*, four Qrr sRNAs (Qrr1-Qrr4) are present that were shown to act redundantly to control bioluminescence, that is, any one of the Qrr sRNAs is sufficient to control HapR (LuxR homolog) (28). In their study, Lenz and colleagues showed that it was not until all four Qrrs were deleted in *V. cholerae*, that there is a difference in density-dependent bioluminescence (28). In *V. harveyi*, the five Qrrs were shown to act additively to control LuxR expression. Using bioluminescence assays and quadruple *qrr* mutants, it was determined that each Qrr has a different level of strength in repressing *luxR* translation (28). In *V. parahaemolyticus*, it appears that expression of *qrr4* is restricted to low cell density cells, since we only observed expression at OD 0.1 and has an absolute requirement for LuxO and RpoN since we did not observed expression in either mutant. It is of interest to note that *qrr1* expression was unchanged in both the *luxO* and *rpoN* mutants at both ODs compared to wild type, which means this *qrr* uses an alternative sigma factor for transcription. We demonstrated that Qrr2 sRNA is the only Qrr that can act alone to control QS gene expression, but is not essential under the conditions examined, since a Δ*qrr2* mutant behaves like wild type (**Fig. S7**). Given that *qrr2* can be transcribed independent of RpoN, this suggests that Qrr2 may have unique functions and/or targets in this species. We propose that *V. parahaemolyticus* can activate the transcription of *qrr2* via RpoN or RpoD to timely alter gene expression likely under different growth conditions. Overall our data suggest that the expression of each *qrr* gene is controlled differently, and likely by a different set of regulators.

Downloaded from https://journals.asm.org/journal/jb on 25 October 2021 by 132.174.254.72.

Journal of Bacteriology

Accepted Manuscript Posted Online

Journal of Bacteriology

JB

Materials and Methods:

Bacterial strains and media. In this study, the wild type (WT) strain is a streptomycin-resistant clinical isolate of *Vibrio parahaemolyticus* RIMD2210633 and all strains used are described in **Table S1** (70, 71). All *V. parahaemolyticus* strains were grown in lysogeny broth (LB; Fisher Scientific, Fair Lawn, NJ) supplemented with 3% NaCl (LBS) (weight/volume). *E. coli* strains were grown in LB 1% NaCl. A diaminopimelic acid (DAP) auxotroph of *E. coli* β2155 *λpir* was grown with 0.3 mM DAP in LB 1% NaCl. All strains were grown aerobically at 37°C. Antibiotics were used in the following concentrations: chloramphenicol (Cm), 12.5 μg/mL, streptomycin (Str), 200 μg/mL; and tetracycline (Tet), 1 μg/mL.

Construction of *V. parahaemolyticus* mutants. We created the double deletion mutants Δ*rpoN*/Δ*luxO* and Δ*rpoN*/Δ*fis* using mutant vectors pDSΔ*luxO* and pDSΔ*fis,* conjugated into the *V. parahaemolyticus* Δ*rpoN* mutant background. The Δ*qrr*-null mutant was constructed by creating truncated, non-functional copies of each *qrr* using splicing by overlap extension (SOE) primer design, with primers listed in **Table S2.** All truncated *qrr* products were cloned into pDS132 suicide vector, transformed into the *E. coli* β2155 *λpir*, followed by conjugation and homologous recombination into the *V. parahaemolyticus* genome. Positive single-cross over colonies were selected using Cm. To induce a double crossover event, a positive single-cross strain was grown overnight in the absence of Cm, leaving behind either the truncated *qrr* allele or the wild-type allele

Journal of Bacteriology

Downloaded from https://journals.asm.org/journal/jb on 25 October 2021 by 132.174.254.72.

Accepted Manuscript Posted Online

Journal of Bacteriology

JB

in the genome. The overnight culture was plated on sucrose plates for selection of normal versus soupy colony morphology, as the colonies still harboring the pDS132Δ*qrr* vector appear irregular due to the *sacB* gene. Colonies were screened via PCR for the truncated allele and sequenced to confirm deletion. The *qrr* null mutant was constructed by deleting qrr genes in the following order: *qrr3*, *qrr2*, *qrr1*, *qrr4*, *qrr5*. The quadruple Δ*qrr3*/Δ*qrr2*/Δ*qrr4*/Δ*qrr5* mutant was constructed by re-introducing *qrr1* into the Δ*qrr*-null mutant, and similarly *qrr2* and *qrr3* were each separately cloned into the Δ*qrr*-null mutant to create their corresponding quad mutants. The Δ*qrr3*/Δ*qrr2*/Δ*qrr1*/Δ*qrr5* mutant was constructed by deleting *qrr5* in the Δ*qrr3*/Δ*qrr2*/Δ*qrr1* mutant background and Δ*qrr3*/Δ*qrr2*/Δ*qrr1*/Δ*qrr4* was constructed by knocking out *qrr4* in the Δ*qrr3*/Δ*qrr2*/Δ*qrr1* background. The Δ*qrr2* single mutant was constructed using the pDSΔ*qrr2* construct conjugated into the wild type background. The Δ*rpoN*/Δ*qrr2* mutant was constructed by conjugating the pDSΔ*qrr2* vector into the Δ*rpoN* background. All mutants were sequenced to confirm deletions or insertions, ensuring in-frame mutant strains.

Complementation analysis of QS mutants. To confirm that the phenotypes observed in the QS mutants were not due to secondary mutations within the genome, the Δ*rpoN* and Δ*opaR* strains were complemented with functional copies of the gene. The *opaR* coding region, plus 33-bp upstream to include the ribosomal binding site, were amplified from *V. parahaemolyticus* RIMD2210633 genome via the Phusion High-Fidelity (HF) polymerase PCR (New England Biolabs). The amplified 670-bp *opaR* coding region

Downloaded from https://journals.asm.org/journal/jb on 25 October 2021 by 132.174.254.72.

Accepted Manuscript Posted Online

Journal of Bacteriology

JB

and pBAD33 empty vector (pBADEV) were digested with XbaI and HindIII restriction enzymes prior to ligation and transformation into *E. coli* β2155. pBAD*opaR* was conjugated into Δ*opaR* and Δ*rpoN* strain. For complementation of the Δ*rpoN* strain with a functional copy of *rpoN,* a similar procedure was followed, however using Gibson assembly. Briefly, a full-length copy of the *rpoN* gene was PCR amplified and cloned into the expression vector pBAD using Gibson assembly primers, transformed into *E. coli*, and conjugated into the Δ*rpoN* strain, designated Δ*rpoN*p*rpoN*. Complementation primers can be found in **Table S2**.

RNA isolation and real-time PCR. *Vibrio parahaemolyticus* wild type and mutants were grown overnight in LBS. Cells were washed twice with 1x phosphate-buffered saline (PBS) and diluted 1:50 into a fresh 5 mL culture of LBS. Cells were harvested at 0.1 OD and 0.5 OD and pelleted at 4°C. RNA was isolated from 4 mL of culture using the miRNAeasy Mini Kit (Qiagen, Hilden, Germany) and Qiazol lysis reagent. The concentration and purity of RNA was determined using a NanoDrop spectrophotometer (Thermo Scientific, Waltham, MA). RNA was treated with Turbo DNase (Invitrogen) and cDNA was synthesized using Superscript IV reverse transcriptase (Invitrogen) from 500 ng of RNA by priming with random hexamers. cDNA was diluted 1:10 for quantitative real-time PCR (qPCR) run on an Applied Biosystems QuantStudio™ 6 fast real-time PCR system (Applied Biosystems, Foster City, CA) using PowerUp SYBR green master mix (Life Technologies). qPCR primers

Downloaded from https://journals.asm.org/journal/jb on 25 October 2021 by 132.174.254.72.

Accepted Manuscript Posted Online

Journal of Bacteriology

JB

used to amplify *opaR*, *aphA*, *qrr1*, *qrr2*, *qrr3*, *qrr4*, *qrr*5, and *16S* rRNA are listed in **Table S2** for reference. Cycle thresholds (C_T) values were used to determine expression levels normalized to 16S rRNA levels. Expression was calculated relative to wild-type 16S rRNA using the $\Delta\Delta C_T$ method (72). Efficiency of the qPCR primers used in this study were determined using a standard curve and calculated to be between 90-110% with melting temps between 55-60°C. In WT and at both 0.1 and 0.5 OD, all five *qrrs* came off between four C_T values of one another. Expression of q*rr4* was undetermined at 0.5 OD in WT and at 0.1 OD and 0.5 OD in Δ*luxO* and Δ*rproN* mutants.

Transcriptional GFP-reporter assay. The P*qrr2* reporter construct was created using the pRU1064 vector, which contains a promoter-less *gfp* cassette, as well as Tet and Amp resistance genes (73). Primers, listed in **Table S2**, were designed using NEBuilder online software to amplify the 337-bp regulatory region of *qrr2* from *V. parahaemolyticus* RIMD2210633 genomic DNA. The pRU1064 vector was purified, digested with Spe1, and ligated with the P*qrr2* fragment via Gibson assembly protocol (74). The plasmid was then transformed into β2155 *λpir* and subsequently conjugated into wild-type and Δ*luxO*, Δ*rpoN,* and Δ*rpoN*/Δ*fis* mutants. Cultures were grown overnight in LBS with 1μg/mL Tet, washed twice with 1xPBS and then diluted 1:1000 into fresh LBS + Tet and grown for 20 hours at 37°C. Cultures were washed twice with 1xPBS and loaded into a black, clear-bottom 96-well plate. Final OD and GFP relative fluoresces were determined using a Tecan Spark microplate reader with Magellan software with

Downloaded from https://journals.asm.org/journal/jb on 25 October 2021 by 132.174.254.72.

Accepted Manuscript Posted Online

Journal of Bacteriology

JB

Journal of Bacteriology

excitation at 385 nm and emission at 509 nm (Tecan Systems, Inc., San Jose, CA). Specific fluorescence was calculated by dividing the relative fluorescence by the final OD. This experiment was performed for three biological replicates.

Splicing by overlap extension (SOE) primer design was used to construct a mutated (ATA-10CCC) RpoD promoter. We used the same SOE*qrr2*A and SOE*qrr2*D primers used to construct the Δ*qrr2* mutant in order to create a mutated *qrr2* regulatory region. In addition, SOE primers P*qrr2*SDMB and P*qrr2*SDMC (**Table S2**) have complementary overlapping sequences that amplify a mutated promoter, indicated in bold. Fragments AB and CD were then used as a template to amplify the AD fragment, containing a mutated RpoD -10 promoter. The AD fragment was then used as the template to create a fragment containing only the *qrr2* regulatory region (337-bp) using Gibson assembly primers P*qrr2*SDM_GAfwd and P*qrr2*SDM_GArev. This mutated regulatory region was then ligated with SpeI digested pRU1064 using Gibson assembly and confirmed via sequencing.

Capsule polysaccharide (CPS) formation assay. Capsule polysaccharide (CPS) formation assays were conducted as previously described (14, 46). In brief, single colonies of wild type and QS mutants were grown on heart infusion (HI) (Remel, Lenexa, KS) plates containing 1.5% agar, 2.5 mM $CaCl_2$, and 0.25% Congo red dye for 48 h at 30°C. Each image is an example from three biological replicates. The pBAD33 expression vector was used to overexpress *opaR* in wild type and Δ*rpoN* backgrounds as

Downloaded from https://journals.asm.org/journal/jb on 25 October 2021 by 132.174.254.72.

Accepted Manuscript Posted Online

Journal of Bacteriology

JB

described in the complementation analysis section. pBAD*opaR* and pBADEV were conjugated into Δ*rpoN* and Δ*opaR* and plated on Congo red plates to observe CPS formation. For strains containing pBAD, 0.1% (wt/vol) L-arabinose and 5 μg/mL of Cm were added to the media after autoclaving, to induce and maintain the plasmid, respectively.

Biofilm assay. *Vibrio parahaemolyticus* cultures were grown overnight in LBS at 37°C with shaking. The overnight cultures were then used to inoculate a 96-well microtiter plate in a 1:50 dilution with LBS. After static incubation at 37°C for 24 h, the culture liquid was removed, and the wells were washed with 1xPBS. Crystal violet (Electron Microscopy Sciences), at 0.1% w/v, was added to the wells and incubated for 30 min at room temperature. The crystal violet was removed, and wells were washed twice with 1xPBS. The adhered crystal violet was solubilized in DMSO for an optical density reading at 595nm (OD_{595}).

Motility assays. Swimming and swarming assays were performed as previously described (14, 57). To assess swimming, a pipette tip was used to pick a single colony and stab into the center of an LB plate containing 2% NaCl and 0.3% agar. Plates were incubated for 24 h at 37°C. Three biological replicates were performed, and the diameter of growth was measured for quantification. Swarming assays were conducted on HI plates containing 2% NaCl and 1.5% agar and incubated at 30°C for 48 h before imaging.

Downloaded from https://journals.asm.org/journal/jb on 25 October 2021 by 132.174.254.72.

Accepted Manuscript Posted Online

Journal of Bacteriology

JB

Phylogenetic analysis. The five *qrr* genes from four species were downloaded from Genbank and aligned using CLUSTALW (75). An evolutionary history was inferred by using the Maximum Likelihood method and Jukes-Cantor model in MEGA X (76, 77). The tree with the highest log likelihood (-467.92) was used. The percentage of trees in which the associated taxa clustered together is shown next to the branches (78). Initial tree(s) for the heuristic search were obtained automatically by applying Neighbor-Join and BioNJ algorithms to a matrix of pairwise distances estimated using the Maximum Composite Likelihood (MCL) approach, and then selecting the topology with superior log likelihood value. A discrete Gamma distribution was used to model evolutionary rate differences among sites (3 categories (+*G*, parameter = 0.2492)). The tree is drawn to scale, with branch lengths measured in the number of substitutions per site. This analysis involved 20 nucleotide sequences.

DNA-affinity pull-down. A DNA-affinity pull-down was performed using previously described methods, with modifications as needed (79-81). Bait DNA primers were designed to amplify the regulatory region of *qrr2* (346-bp) with a biotin moiety added to the 5′ end. In addition, a negative control bait DNA (VPA1624 coding region, 342-bp) was amplified. Both bait DNA probes were amplified using Phusion HF polymerase (New England Biolabs) PCR and purified using ethanol extraction techniques (82). A 5 mL overnight culture of Δ*rpoN* grown in LB 3% NaCl was used to inoculate a fresh 100 mL culture of LB 3% NaCl grown at 37˚C with aeration. The culture was pelleted at 0.5 OD at 4°C for 30 min and stored overnight at 80˚C. The cell pellet was suspended in 1.5 mL of Fastbreak lysis buffer (Promega, Madison, WI) and sonicated to shear genomic

Downloaded from https://journals.asm.org/journal/jb on 25 October 2021 by 132.174.254.72.

Accepted Manuscript Posted Online

Journal of Bacteriology

JB

Journal of Bacteriology

493 DNA. The Δ*rpoN* lysate was pre-cleared with streptavidin DynaBeads (Thermo
494 Scientific, Waltham, MA) to remove non-specific protein-bead interactions. Beads were
495 incubated with 200 µL of probe DNA for 20 min, twice. The Δ*rpoN* lysate and sheared
496 salmon sperm DNA (10µg/mL), as competitive DNA, were incubated with the beads
497 twice, and washed. Protein candidates were eluted from the bait DNA-bead complex
498 using elution buffers containing increasing concentrations of NaCl (100mM, 200mM,
499 300mM, 500mM, 750mM and 1M). 6X SDS was added to samples along with 1mM β-
500 mercaptoethanol (BME) and then boiled at 95°C for 5 min. A total of 25 µL of each
501 elution was run on 2 stain-free, 12% gels and visualized using the Pierce™ Silver Stain
502 for Mass Spectrometry kit (Thermo Scientific, Waltham, MA). P*qrr2* bait and negative
503 control bait were loaded next to each other in order of increasing NaCl concentrations.
504 Bands present in the P*qrr2* bait lanes, but not in the negative control lanes were selected
505 and cut from the gel. Each fragment was digested separately with trypsin using
506 standard procedures and prepared for Mass Spectrophotometry 18C ZipTips (Fisher
507 Scientific, Fair Lawn, NJ). Candidates were eluted in 10 µL twice, pooled, and dried
508 again using SpeedVac. Dried samples were analyzed using the Thermo Q-Exactive
509 Orbitrap and analyzed using Proteome Discoverer 1.4.
510 **Fis protein purification**. Fis was purified using the method previously described (59).
511 Briefly, primer pair FisFWDpMAL and FisREVpMAL was used to amplify *fis* (VP2885)
512 from *V. parahaemolyticus* RIMD2210633. The *fis* gene was cloned into the pMAL-c5x

Downloaded from https://journals.asm.org/journal/jb on 25 October 2021 by 132.174.254.72.

Accepted Manuscript Posted Online

Journal of Bacteriology

JB

Journal of Bacteriology

513 expression vector fused to a 6X His tag maltose binding protein (MBP) separated by a
514 tobacco etch virus (TEV) protease cleavage site. Expression of pMAL*fis* in *E. coli* BL21
515 (DE3) was induced with 0.5 mM IPTG once the culture reached 0.4 OD_{595} and grown
516 overnight at room temperature. Cells were harvested, suspended in lysis buffer (50 mM
517 NaPO4, 200 mM NaCl, and 20 mM imidazole buffer [pH 7.4]), and lysed using a
518 microfluidizer. The lysed culture was subject to Immobilized Metal Affinity
519 Chromatography (IMAC) using HisPur Ni-NTA resin, followed by additional washing
520 steps. After purification, the MBP tag was cleaved overnight at 4° C with a
521 hexahistidine-tagged Tobacco Etch Virus (TEV) protease in a 1:10 molar ratio. Mass
522 spectrometry was performed to confirm Fis protein molecular weight and SDS-PAGE
523 was conducted to determine its purity along with A260/280 ratio analysis using a
524 NanoDrop.
525 **Electrophoretic mobility shift assay for Fis.** Purified Fis was used to conduct EMSAs
526 using conditions previously described (55, 59). Briefly, 30 ng of DNA probe was
527 incubated with various concentrations of Fis (0 to 1.94 μM) in binding buffer (10 mM
528 Tris, 150 mM KCL, 0.1 mM dithiothreitol, 0.1 mM EDTA, 5% PEG, pH7.4) for 20 min.
529 The concentration of Fis was determined using Bradford reagent. A 6% native
530 polyacrylamide gel was pre-run for 2 h at 4°C (200V) with 1x Tris-acetate-EDTA (TAE)
531 buffer. The incubated DNA-protein samples were then loaded onto the gel (10 μL) and
532 run for 2 h in the same conditions. The gel was stained in an ethidium bromide bath

Downloaded from https://journals.asm.org/journal/jb on 25 October 2021 by 132.174.254.72.

(0.5μg/mL) for 15 min before imaging. P*qrr2* was further divided into a smaller probe to determine specificity of Fis binding to P*qrr2*.

Acknowledgments

We thank the three anonymous reviewers for their constructive suggestions and comments. This research was supported by a National Science Foundation grant (award IOS-1656688) to E.F.B. J.G.T was funded by University of Delaware graduate fellowship award.

Accepted Manuscript Posted Online
Journal of Bacteriology
JB
Journal of Bacteriology
Downloaded from https://journals.asm.org/journal/jb on 25 October 2021 by 132.174.254.72.

Accepted Manuscript Posted Online

1. Fuqua WC, Winans SC, Greenberg EP. 1994. Quorum sensing in bacteria: the LuxR-LuxI family of cell density-responsive transcriptional regulators. J Bacteriol 176:269-75.
2. Swift S, Downie J, Whitehead N, Barnard A, Salmond G, P W. 2001. Quorum sensing as a population-density-dependent determinant of bacterial physiology. Adv Microb Physiol 45:199-270.
3. Gray KM, Passador L, Iglewski BH, Greenberg EP. 1994. Interchangeability and specificity of components from the quorum-sensing regulatory systems of *Vibrio fischeri* and *Pseudomonas aeruginosa*. J Bacteriol 176:3076-80.
4. Nealson KH, Platt T, Hastings JW. 1970. Cellular control of the synthesis and activity of the bacterial luminescent system1. J Bacteriol 104:313-22.
5. Miller MB, Skorupski K, Lenz DH, Taylor RK, Bassler BL. 2002. Parallel quorum sensing systems converge to regulate virulence in *Vibrio cholerae*. Cell 110:303-14.
6. Miller MB, Bassler BL. 2001. Quorum sensing in bacteria. Annu Rev Microbiol 55:165-99.
7. Bassler BL, Greenberg EP, Stevens AM. 1997. Cross-species induction of luminescence in the quorum-sensing bacterium *Vibrio harveyi*. J Bacteriol 179:4043-5.
8. Lilley BN, Bassler BL. 2000. Regulation of quorum sensing in *Vibrio harveyi* by LuxO and sigma-54. Mol Microbiol 36:940-54.
9. Egland KA, Greenberg EP. 1999. Quorum sensing in *Vibrio fischeri*: elements of the luxl promoter. Mol Microbiol 31:1197-204.
10. Dunlap PV. 1999. Quorum regulation of luminescence in *Vibrio fischeri*. J Mol Microbiol Biotechnol 1:5-12.
11. Camara M, Hardman A, Williams P, Milton D. 2002. Quorum sensing in *Vibrio cholerae*. Nat Genet 32:217-8.
12. Zhu J, Miller MB, Vance RE, Dziejman M, Bassler BL, Mekalanos JJ. 2002. Quorum-sensing regulators control virulence gene expression in *Vibrio cholerae*. Proc Natl Acad Sci U S A 99:3129-34.
13. Bassler BL, Wright M, Showalter RE, Silverman MR. 1993. Intercellular signaling in *Vibrio harveyi*: sequence and function of genes regulating expression of luminescence. Mol Microbiol 4:773-86.
14. Kalburge SS, Carpenter MR, Rozovsky S, Boyd EF. 2017. Quorum sensing regulators are required for metabolic fitness in *Vibrio parahaemolyticus*. Infect Immun 85:930-16.
15. Kernell Burke A, Guthrie LTC, Modise T, Cormier G, Jensen RV, McCarter LL, Stevens AM. 2015. OpaR controls a network of downstream transcription factors in *Vibrio parahaemolyticus* BB22OP. PLoS One 10.

Journal of Bacteriology JB Journal of Bacteriology

Downloaded from https://journals.asm.org/journal/jb on 25 October 2021 by 132.174.254.72.

Accepted Manuscript Posted Online

16. Zhang Y, Qiu Y, Tan Y, Guo Z, Yang R, Zhou D. 2012. Transcriptional regulation of opaR, qrr2-4 and aphA by the master quorum-sensing regulator OpaR in *Vibrio parahaemolyticus*. PLoS One 7:e34622.
17. Trimble MJ, McCarter LL. 2011. Bis-(3'-5')-cyclic dimeric GMP-linked quorum sensing controls swarming in *Vibrio parahaemolyticus*. Proc Natl Acad Sci U S A 108:18079-84.
18. Sun F, Zhang Y, Wang L, Yan X, Tan Y, Guo Z, Qiu J, Yang R, Xia P, Zhou D. 2012. molecular characterization of direct target genes and cis-acting consensus recognized by quorum-sensing regulator AphA in *Vibrio parahaemolyticus*. PLoS One 7:e44210.
19. Zhang Y, Zhang L, Hou S, Huang X, Sun F, Gao H. 2016. The master quorum-sensing regulator OpaR is activated indirectly by H-NS in *Vibrio parahaemolyticus*. Curr Microbiol 73:71-6.
20. Enos-Berlage JL, Guvener ZT, Keenan CE, McCarter LL. 2005. Genetic determinants of biofilm development of opaque and translucent *Vibrio parahaemolyticus*. Mol Microbiol 55:1160-82.
21. Lin B, Wang Z, Malanoski AP, O'Grady EA, Wimpee CF, Vuddhakul V, Alves N, Jr., Thompson FL, Gomez-Gil B, Vora GJ. 2010. Comparative genomic analyses identify the Vibrio harveyi genome sequenced strains BAA-1116 and HY01 as *Vibrio campbellii*. Environ Microbiol Rep 2:81-89.
22. Weber B, Lindell K, El Qaidi S, Hjerde E, Willassen N, Milton D. 2011. The phosphotransferase VanU represses expression of four *qrr* genes antagonizing VanO-mediated quorum-sensing regulation in *Vibrio anguillarum*. Microbiology 157:3324-3339.
23. Weber B, Croxatto A, Chen C, Milton D. 2008. RpoS induces expression of the *Vibrio anguillarum* quorum-sensing regulator VanT. Microbiology 154:767-780.
24. Waters LS, Storz G. 2009. Regulatory RNAs in Bacteria. Cell 136:615-28.
25. Storz G, Vogel J, Wassarman KM. 2011. Regulation by small RNAs in bacteria: expanding frontiers. Mol Cell 43:880-91.
26. Updegrove T, Zhang A, Storz G. 2016. Hfq: the flexible RNA matchmaker. Curr Opin Microbiol 30:133-138.
27. Lenz DH, Mok KC, Lilley BN, Kulkarni RV, Wingreen NS, Bassler BL. 2004. The small RNA chaperone Hfq and multiple small RNAs control quorum sensing in *Vibrio harveyi* and *Vibrio cholerae*. Cell 118:69-82.
28. Tu KC, Bassler BL. 2007. Multiple small RNAs act additively to integrate sensory information and control quorum sensing in *Vibrio harveyi*. Genes Dev 21:221-33.
29. Tu KC, Long T, Svenningsen SL, Wingreen NS, Bassler BL. 2010. Negative feedback loops involving small regulatory RNAs precisely control the *Vibrio harveyi* quorum-sensing response. Mol Cell 37:567-79.

Journal of Bacteriology
JB
Journal of Bacteriology
Downloaded from https://journals.asm.org/journal/jb on 25 October 2021 by 132.174.254.72.

Accepted Manuscript Posted Online

30. Lenz DH, Bassler BL. 2007. The small nucleoid protein Fis is involved in *Vibrio cholerae* quorum sensing. Mol Microbiol 63:859-71.
31. Papenfort K, Bassler BL. 2016. Quorum sensing signal-response systems in Gram-negative bacteria. Nat Rev Microbiol 14:576-88.
32. Shao Y, Bassler BL. 2012. Quorum-sensing non-coding small RNAs use unique pairing regions to differentially control mRNA targets. Mol Microbiol 83:599-611.
33. Svenningsen S. 2018. Small RNA-based regulation of bacterial quorum sensing and biofilm formation. Microbiol Spectr 6.
34. Lin W, Kovacikova G, Skorupski K. 2007. The quorum sensing regulator HapR downregulates the expression of the virulence gene transcription factor AphA in *Vibrio cholera*e by antagonizing Lrp- and VpsR-mediated activation. Mol Microbiol 64:953-67.
35. Pompeani AJ, Irgon JJ, Berger MF, Bulyk ML, Wingreen NS, Bassler BL. 2008. The *Vibrio harveyi* master quorum-sensing regulator, LuxR, a TetR-type protein is both an activator and a repressor: DNA recognition and binding specificity at target promoters. Mol Microbiol 70:76-88.
36. Rutherford ST, van Kessel JC, Shao Y, Bassler BL. 2011. AphA and LuxR/HapR reciprocally control quorum sensing in Vibrios. Genes Dev 25:397-408.
37. Shao Y, Feng L, Rutherford S, Papenfort K, Bassler B. 2013. Functional determinants of the quorum-sensing non-coding RNAs and their roles in target regulation. EMBO J 32:2158-71.
38. Hunter GA, Keener JP. 2014. Mechanisms underlying the additive and redundant Qrr phenotypes in *Vibrio harvey*i and *Vibrio cholerae*. J Theor Biol 340:38-49.
39. Joseph S, Colwell R, Kaper J. 1982. *Vibrio parahaemolyticus* and related halophilic Vibrios. Crit Rev Microbiol 10:77-124.
40. Colwell R, Kaper J, Joseph S. 1977. *Vibrio cholerae*, *Vibrio parahaemolyticus*, and other Vibrios: occurrence and distribution in Chesapeake Bay. Science 198:394-6.
41. Thompson F, Iida T, Swings J. 2004. Biodiversity of Vibrios. Microbiol Mol Biol Rev 68:403-31.
42. Nair GB, Ramamurthy T, Bhattacharya SK, Dutta B, Takeda Y, Sack DA. 2007. Global dissemination of *Vibrio parahaemolyticus* serotype O3:K6 and its serovariants. Clin Microbiol Rev 20:39-48.
43. O'Boyle N, Boyd A. 2014. Manipulation of intestinal epithelial cell function by the cell contact-dependent type III secretion systems of *Vibrio parahaemolyticus*. Front Cell Infect Microbiol 3.
44. Allison C, Hughes C. 1991. Bacterial swarming: an example of prokaryotic differentiation and multicellular behaviour. Sci Prog 75:403-22.
45. McCarter LL. 1998. OpaR, a homolog of *Vibrio harveyi* LuxR, controls opacity of *Vibrio parahaemolyticus*, p 3166-73, J Bacteriol, vol 180.

Journal of Bacteriology JB Journal of Bacteriology

Downloaded from https://journals.asm.org/journal/jb on 25 October 2021 by 132.174.254.72.

Accepted Manuscript Posted Online

46. Güvener Z, McCarter L. 2003. Multiple regulators control capsular polysaccharide production in *Vibrio parahaemolyticus*. J Bacteriol 185:5431-41.
47. Zhang Y, Qiu Y, Gao H, Sun J, Li X, Zhang M, Xue X, Yang W, Ni B, Hu L, Yin Z, Lu R, Zhou D. 2021. OpaR controls the metabolism of c-di-GMP in *Vibrio parahaemolyticus*. Front Microbiol 12:676436.
48. Zhong X, Lu R, Liu F, Ye J, Zhao J, Wang F, Yang M. 2021. Identification of LuxR family regulators that integrate into quorum sensing circuit in *Vibrio parahaemolyticus*. Front Microbiol 12:691842.
49. Yildiz FH, Visick KL. 2009. Vibrio biofilms: so much the same yet so different. Trends Microbiol 17:109-18.
50. Lee KJ, Kim JA, Hwang W, Park SJ, Lee KH. 2013. Role of capsular polysaccharide (CPS) in biofilm formation and regulation of CPS production by quorum-sensing in *Vibrio vulnificus*. Mol Microbiol 90:841-57.
51. Lee KJ, Jung YC, Park SJ, Lee KH. 2018. Role of heat shock proteases in quorum-sensing-mediated regulation of biofilm formation by Vibrio species. mBio 9.
52. Joseph LA, Wright AC. 2004. Expression of *Vibrio vulnificus* capsular polysaccharide inhibits biofilm formation. J Bacteriol 186:889-93.
53. Gode-Potratz CJ, McCarter LL. 2011. Quorum sensing and silencing in *Vibrio parahaemolyticus*. J Bacteriol 193:4224-37.
54. Jaques S, McCarter L. 2006. Three new regulators of swarming in *Vibrio parahaemolyticus*. J Bacteriol 188:2625-35.
55. Gregory GJ, Morreale DP, Carpenter MR, Kalburge SS, Boyd EF. 2019. Quorum sensing regulators AphA and OpaR control expression of the operon responsible for biosynthesis of the compatible solute ectoine. Appl Environ Microbiol 85:1543-19.
56. Gregory GJ, Morreale DP, Boyd EF. 2020. CosR is a global regulator of the osmotic stress response with widespread distribution among bacteria. Appl Environ Microbiol 86:120-20.
57. Whitaker WB, Richards GP, Boyd EF. 2014. Loss of sigma factor RpoN increases intestinal colonization of *Vibrio parahaemolyticus* in an adult mouse model. Infect Immun 82:544-56.
58. Eickhoff M, Fei C, Huang X, Bassler B. 2021. LuxT controls specific quorum-sensing-regulated behaviors in Vibrionaceae spp. via repression of *qrr1*, encoding a small regulatory RNA. PLoS Genet 17:e1009336.
59. Tague JG, Regmi A, Gregory GJ, Boyd EF 2021. Fis connects two sensory pathways, quorum sensing and surface sensing, to control motility in *Vibrio parahaemolyticus*. Front Microbiol.
60. Schaefer J, Engl C, Zhang N, Lawton E, Buck M. 2015. Genome wide interactions of wild-type and activator bypass forms of σ54. Nucleic Acids Res 43:7280-91.

Journal of Bacteriology JB Journal of Bacteriology

Downloaded from https://journals.asm.org/journal/jb on 25 October 2021 by 132.174.254.72.

Accepted Manuscript Posted Online

61. Zafar MA, Carabetta VJ, Mandel MJ, Silhavy TJ. 2014. Transcriptional occlusion caused by overlapping promoters. Proc Natl Acad Sci U S A 111:1557-61.
62. Reichenbach B, Göpel Y, Görke B. 2009. Dual control by perfectly overlapping sigma 54- and sigma 70- promoters adjusts small RNA GlmY expression to different environmental signals. Mol Microbiol 74:1054-70.
63. Campbell EA, Kamath S, Rajashankar KR, Wu M, Darst SA. 2017. Crystal structure of *Aquifex aeolicus* σ(N) bound to promoter DNA and the structure of σ(N)-holoenzyme. Proc Natl Acad Sci U S A 114:E1805-e1814.
64. Buck M, Cannon W. 1992. Specific binding of the transcription factor sigma-54 to promoter DNA. Nature 358:422-4.
65. Keane OM, Dorman CJ. 2003. The *gyr* genes of *Salmonella enterica* serovar Typhimurium are repressed by the factor for inversion stimulation, Fis. Mol Genet Genomics 270:56-65.
66. Browning DF, Grainger DC, Beatty CM, Wolfe AJ, Cole JA, Busby SJ. 2005. Integration of three signals at the *Escherichia coli nrf* promoter: a role for Fis protein in catabolite repression. Mol Microbiol 57:496-510.
67. Kelly A, Goldberg MD, Carroll RK, Danino V, Hinton JCD, Dorman CJ. 2004. A global role for Fis in the transcriptional control of metabolism and type III secretion in *Salmonella enterica* serovar Typhimurium. Microbiol 150:2037-2053.
68. Grainger DC, Hurd D, Goldberg MD, Busby SJ. 2006. Association of nucleoid proteins with coding and non-coding segments of the *Escherichia coli* genome. Nucleic Acids Res 34:4642-52.
69. Wang Q, Liu Q, Ma Y, Rui H, Zhang Y. 2007. LuxO controls extracellular protease, haemolytic activities and siderophore production in fish pathogen *Vibrio alginolyticus*. J Appl Microbiol 103:1525-34.
70. Makino K, Oshima K, Kurokawa K, Yokoyama K, Uda T, Tagomori K, Iijima Y, Najima M, Nakano M, Yamashita A, Kubota Y, Kimura S, Yasunaga T, Honda T, Shinagawa H, Hattori M, Iida T. 2003. Genome sequence of *Vibrio parahaemolyticus*: a pathogenic mechanism distinct from that of *V. cholerae*. Lancet 361:743-9.
71. Whitaker WB, Parent MA, Naughton LM, Richards GP, Blumerman SL, Boyd EF. 2010. Modulation of responses of *Vibrio parahaemolyticus* O3:K6 to pH and temperature stresses by growth at different salt concentrations. Appl Environ Microbiol 76:4720-9.
72. Livak KJ, Schmittgen TD. 2001. Analysis of relative gene expression data using real-time quantitative PCR and the 2(-Delta Delta C(T)) Method. Methods 25:402-8.
73. Karunakaran R, Mauchline TH, Hosie AH, Poole PS. 2005. A family of promoter probe vectors incorporating autofluorescent and chromogenic reporter proteins for studying gene expression in Gram-negative bacteria. Microbiol 151:3249-56.

Journal of Bacteriology JB Journal of Bacteriology

Downloaded from https://journals.asm.org/journal/jb on 25 October 2021 by 132.174.254.72.

Accepted Manuscript Posted Online

74. Gibson DG. 2011. Enzymatic assembly of overlapping DNA fragments. Methods Enzymol 498:349-61.
75. Chenna R, Sugawara H, Koike T, Lopez R, Gibson TJ, Higgins DG, Thompson JD. 2003. Multiple sequence alignment with the Clustal series of programs. Nucleic Acids Res 31:3497-500.
76. Jukes TH, Cantor CR. 1969. Evolution of Protein Molecules, p 21-132, Mammalian Protein Metabolism.
77. Kumar S, Stecher G, Li M, Knyaz C, Tamura K. 2018. MEGA X: Molecular evolutionary genetics analysis across computing platforms. Molecular biology and evolution 35:1547-1549.
78. Felsenstein J. 1985. Confidence limits on phylogenies: an approach using the bootstrap. Evolution; international journal of organic evolution 39:1558-5646.
79. Chaparian RR, Tran MLN, Conrad LCM, Rusch DB, Kessel JCv. 2019. Global H-NS counter-silencing by LuxR activates quorum sensing gene expression. Nucleic Acids Res 48:171-83.
80. Chaparian RR, Olney SG, Hustmyer CM, Rowe-Magnus DA, van Kessel JC. 2016. Integration host factor and LuxR synergistically bind DNA to coactivate quorum-sensing genes in *Vibrio harveyi*. Mol Microbiol 101:823-40.
81. Jutras BL, Verma A, Stevenson B. 2012. Identification of novel DNA-binding proteins using DNA-affinity chromatography/pull down. Curr Protoc Microbiol Chapter 1:Unit1F.1.
82. Chaparian RR, van Kessel JC. 2021. Promoter Pull-Down Assay: A Biochemical Screen for DNA-Binding Proteins. Methods Mol Biol 2346:165-172.

Journal of Bacteriology
JB
Journal of Bacteriology
Downloaded from https://journals.asm.org/journal/jb on 25 October 2021 by 132.174.254.72.

Accepted Manuscript Posted Online

Journal of Bacteriology

JB

Journal of Bacteriology

781 **Figure legends**

782

783 **Figure 1**. *Vibrio parahaemolyticus* quorum sensing pathway. Autoinducers (AIs) are
784 synthesizes internally by three synthases and then excreted outside the cell. At low cell
785 density, three histidine-kinase receptors are free of AIs, therefore act as kinases,
786 phosphorylating LuxU and ultimately LuxO. LuxO-P activates RpoN and, along with
787 Fis positively regulates transcription of five small quorum regulatory RNAs (Qrr
788 sRNAs). The Qrr sRNAs, along with Hfq, stabilize *aphA* transcripts and destabilize *opaR*
789 transcripts. In addition, AphA is a negative regulator of *opaR* expression. At high cell
790 density, LuxO is unphosphorylated and inactivate, no *qrrs* are transcribed, *opaR* is
791 expressed and *aphA* is repressed. OpaR positively regulates capsule polysaccharide
792 production (CPS), biofilm formation, type 6 secretion system-1, and the type IV pilin
793 MSHA, among other genes. OpaR negatively regulates swarming motility, surface
794 sensing and two contact dependent secretion systems T3SS-1 and T6SS-1.
795 **Figure 2.** Quorum sensing phenotypes**. A.** Wild type (WT) and QS mutant strains
796 production of capsule polysaccharide (CPS) and colony morphology on Congo red
797 plates. **B**. Biofilm assay from cultures grown for 24 h, stagnant and stained with crystal
798 violet. Images are representatives from three bio-reps. Biofilm quantification of three
799 bio-reps in duplicate. Statistics calculated using a Student's t-test. ***, P-value <0.001
800 **Figure 3.** Quantitative real time PCR expression analysis of cells grown to 0.1 (**A, C)** or
801 0.5 OD (**B, D)** in LB media supplemented with 3% NaCl. Bars represent the expression
802 of *opaR* and *aphA* in Δ*luxO* and Δ*rpoN* mutants normalized to the expression of 16S
803 rRNA housekeeping gene, relative to expression in wild type. Means and standard
804 error of at least two biological replicates shown. Statistics calculated using a Student's t-
805 test. *, P-value <0.05; **, P-value <0.01.
806 **Figure 4.** Quantitative real time PCR (qPCR) analysis of cells grown to OD 0.1 (**A, C**) or
807 OD 0.5 (**B, D**) in LB media supplemented with 3% NaCl. Expression of *qrr1* to *qrr5* in
808 the Δ*luxO* and Δ*rpoN* mutants, relative to wild type RIMD2210633 and normalized to
809 16S rRNA housekeeping gene, relative to wild type expression of each gene. Expression
810 of *qrr4* not detected in mutant strains. Means and standard error of at least two
811 biological replicates shown. Statistics calculated using a Student's t-test. *, P-value <0.05;
812 **, P-value <0.01; ***, P-value <0.001.
813 **Figure 5.** Expression analysis of *qrr2.* **A.** P*qrr2*-gfp reporter assay of *qrr2* in Δ*luxO* and
814 Δ*rpoN* mutants. **B**. P*opaR*-gfp reporter assays in a single qrr2 deletion mutant and a
815 quadruple mutant with only *qrr2* present. Cultures grown for 20 h in LB 3% NaCl.
816 Means and standard error of at least three biological replicates shown. Statistics
817 calculated using a one-way ANOVA and Tukey-Kramer *post-hoc* test. **, P-value <0.01

Downloaded from https://journals.asm.org/journal/jb on 25 October 2021 by 132.174.254.72.

Accepted Manuscript Posted Online

Journal of Bacteriology

JB

Figure 6. *qrr2* promoter analysis. **A.** Analysis of *qrr2* regulatory region indicates overlapping sigma-54 and sigma-70 promoters. **B.** P*qrr2* GFP reporter assay of *qrr2* in Δ*rpoN* relative to wild type and mutated putative -10 RpoD binding site are indicated by asterisks. Means and standard error of three biological replicates shown. Statistics calculated using a one-way ANOVA and Tukey-Kramer *post-hoc* test. ***, P-value <0.001

Figure 7. Phylogenetic tree of the *qrr* genes from *V. harveyi* ATCC 33843, *V. campbellii* ATCC BAA-1116 (formerly *V. harveyi*), *V. parahaemolyticus* RIMD2210633 *and V. alginolyticus* FDAARGOS_114. The numbers along the branches indicate bootstrap values. The tree is drawn to scale, with branch lengths measured in the number of substitutions per site. This analysis involved 20 nucleotide sequences.

Figure 8. Phenotypes of *qrr* deletion mutants. **A.** Swarming assay conducted on heart-infusion media incubated at 30˚C for 48 hrs. **B.** Swimming motility assay conduced on semi-solid agar plates grown at 37˚C for 24 hrs. Swimming plate quantification of three biological replicates. Statistics calculated using Student's t-test relative to Wild-type. ***, P-value <0.001. **C.** CPS assays conducted of strains of interest. Colonies grown on Congo red plates for 48 hrs at 30˚C prior to imaging.

Figure 9. Fis binding in the *qrr2* regulatory region. **A.** Regulatory region of *qrr2* depicted. Lines represent EMSA probes and blue triangles represent putative Fis binding sites using Virtual Footprint prediction software. Numbers indicate Fis binding site distance from *qrr2* transcriptional start site. **B.** Electrophoretic mobility shift assays of P*qrr2* with purified Fis protein using three *qrr2* regulatory region DNA probes **C.** pRUP*qrr2* reporter assays in Δ*rpoN* and Δ*rpoN*/Δ*fis* deletion mutants relative to WT. Cultures grown for 20 h in LB 3% NaCl. Means and standard error of at least three biological replicates shown. Statistics calculated using a one-way ANOVA and Tukey-Kramer *post-hoc* test. ***, P-value <0.001.

Figure 10. Model for *qrr2* transcription in the Δ*luxO* and Δ*rpoN* mutants. In the Δ*luxO* mutant, under certain conditions RpoN will be bound to the *qrr2* RpoN -24 -12 promoter region. RpoN bound at the promoter will be aided by Fis. This will prevent sigma-70 from binding. In the absence of RpoN (sigma-54), RpoD (sigma-70) can bind to the -35 -10 promoter region to initiate transcription. In the absence of Fis in the Δ*rpoN* mutant transcription by RpoD is increased further as in the Δ*rpoN*/Δ*fis* mutant, which suggests Fis may block RpoD binding in exponential phase cells.

Downloaded from https://journals.asm.org/journal/jb on 25 October 2021 by 132.174.254.72.

Accepted Manuscript Posted Online

Journal of Bacteriology

JB

Journal of Bacteriology

Downloaded from https://journals.asm.org/journal/jb on 25 October 2021 by 132.174.254.72.

Accepted Manuscript Posted Online

Journal of Bacteriology

JB

Journal of Bacteriology

A. CPS production and colony morphology in QS mutants

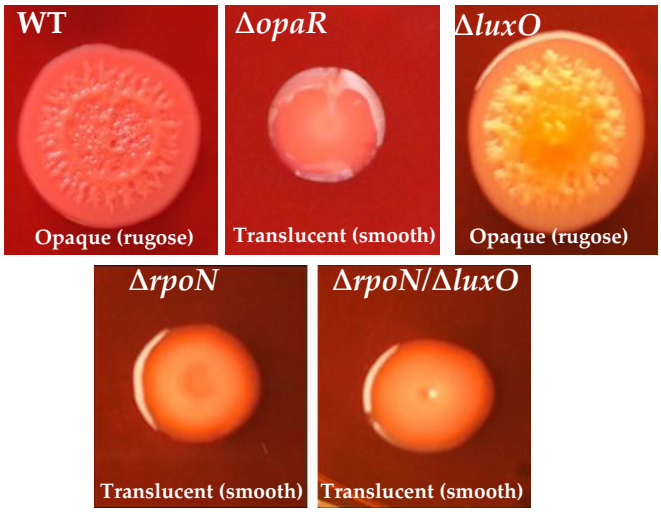

B. Biofilm quantification of QS mutants

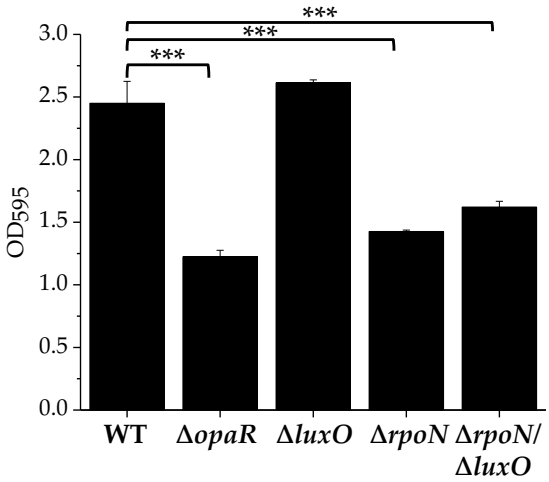

Downloaded from https://journals.asm.org/journal/jb on 25 October 2021 by 132.174.254.72.

Accepted Manuscript Posted Online

Journal of Bacteriology

JB

Journal of Bacteriology

A. ***opaR*** **expression OD 0.1**

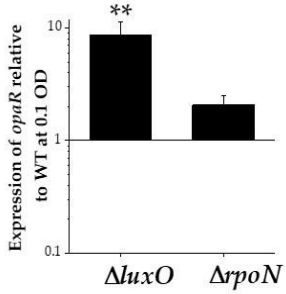

B. ***opaR*** **expression OD 0.5**

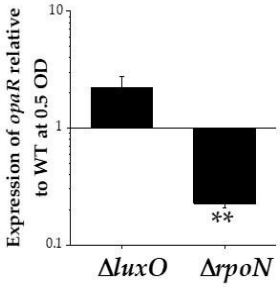

C. ***aphA*** **expression OD 0.1**

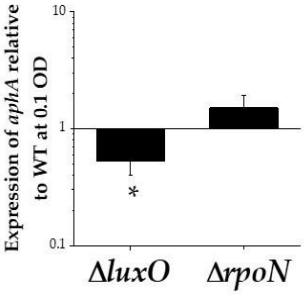

D. ***aphA*** **expression OD 0.5**

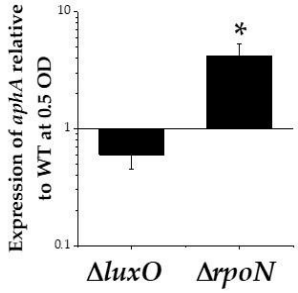

Downloaded from https://journals.asm.org/journal/jb on 25 October 2021 by 132.174.254.72.

Accepted Manuscript Posted Online

Journal of Bacteriology

JB

Journal of Bacteriology

A. Qrr sRNA gene expression in Δ*luxO* OD 0.1

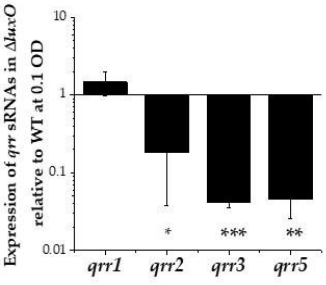

B. Qrr sRNA gene expression in Δ*luxO* OD 0.5

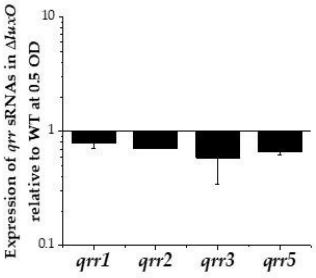

C. Qrr sRNA gene expression in Δ*rpoN* OD 0.1

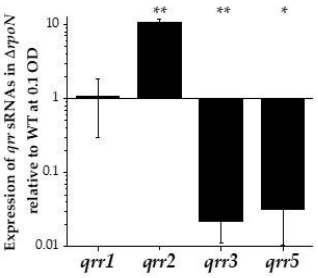

D. Qrr sRNA gene expression in Δ*rpoN* OD 0.5

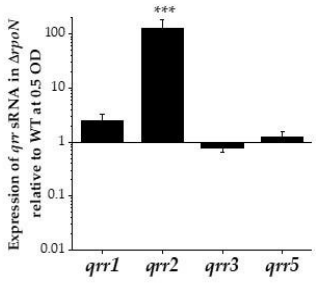

Downloaded from https://journals.asm.org/journal/jb on 25 October 2021 by 132.174.254.72.

Accepted Manuscript Posted Online

Journal of Bacteriology

JB

Journal of Bacteriology

A. P*qrr2-gfp* expression in Δ*luxO* and Δ*rpoN* mutants

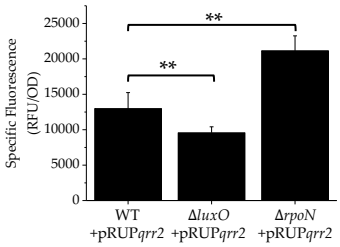

B. P*opaR-gfp* expression in Δ*qrr2* mutant and quadruple Δ*qrr1,3,4,5* mutant

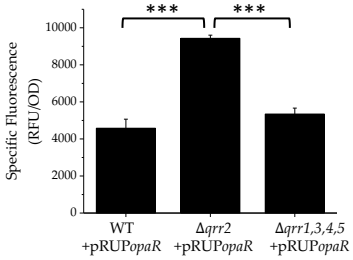

Downloaded from https://journals.asm.org/journal/jb on 25 October 2021 by 132.174.254.72.

Accepted Manuscript Posted Online

Journal of Bacteriology

JB

Journal of Bacteriology

A. Putative sigma-70 -10 -35 promoter present in *qrr2* regulatory region

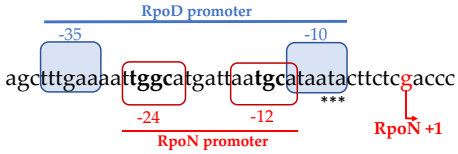

B. Mutation of putative sigma-70 -10 promoter site and expression of *qrr2*

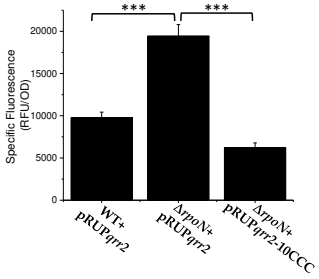

Downloaded from https://journals.asm.org/journal/jb on 25 October 2021 by 132.174.254.72.

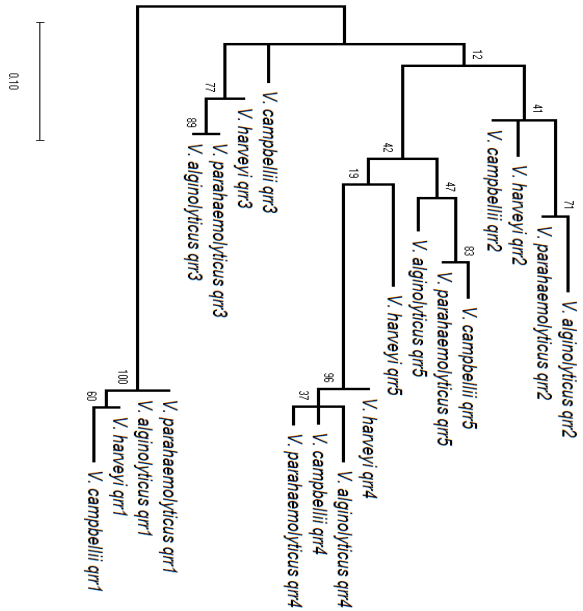

Downloaded from https://journals.asm.org/journal/jb on 25 October 2021 by 132.174.254.72.

Accepted Manuscript Posted Online
Journal of Bacteriology
JB
Journal of Bacteriology

A. Swarming motility in *qrr* deletion mutants

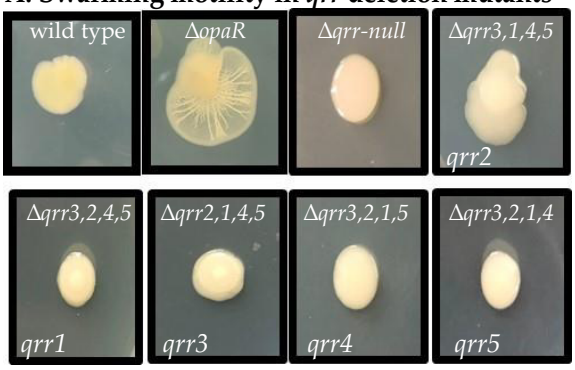

B. Swimming motility in *qrr* deletion mutants

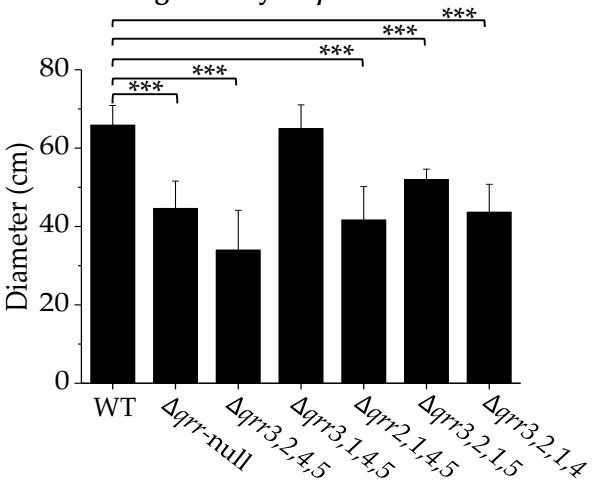

C. Capsule polysaccharide production among *qrr* deletion mutants

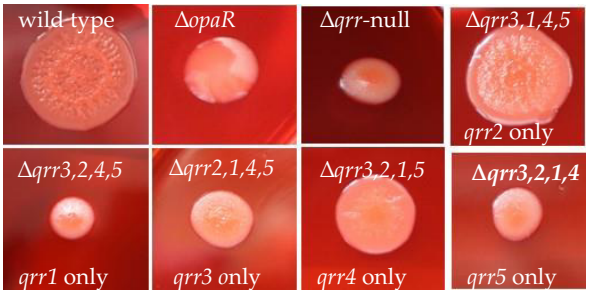

Downloaded from https://journals.asm.org/journal/jb on 25 October 2021 by 132.174.254.72.

Accepted Manuscript Posted Online

Journal of Bacteriology

JB

Journal of Bacteriology

A. Fis binding sites present in *qrr2* regulatory region

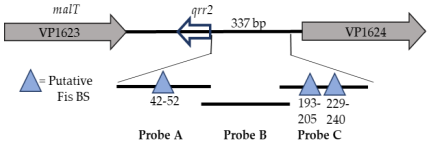

B. Electrophoretic mobility shift assays of P*qrr2*

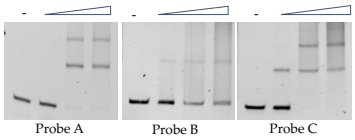

C. RpoN and Fis repress *qrr2* transcription

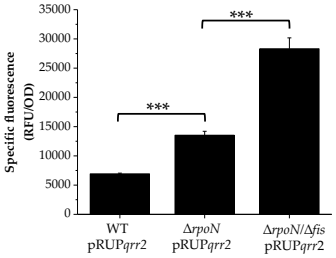

Downloaded from https://journals.asm.org/journal/jb on 25 October 2021 by 132.174.254.72.

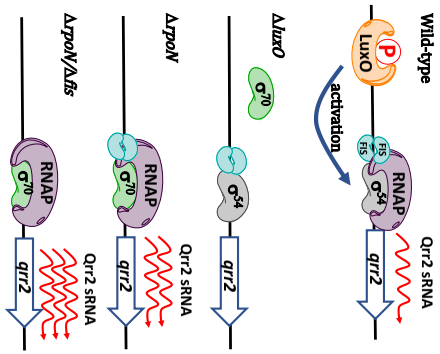

Downloaded from https://journals.asm.org/journal/jb on 25 October 2021 by 132.174.254.72.